SPE Flow Assurance Technology Congress
Rio de Janeiro, Brazil, November 15 – 18 2022

# Wellhead Hydrate Deposition and Hydrate Management in Gas Wells

Yohan Lee[1], Amadeu K. Sum[1*], Taras Y. Makogon[2]
[1] Phases to Flow Laboratory, Colorado School of Mines, Golden (USA)
[2] Saudi Aramco, Dhahran (KSA)
[*]asum@mines.edu

## Abstract
Wellheads are susceptible to hydrate formation which is of particular concern due to the possible plugging of the well tubing line, resulting in significant operational loss in additional of creating potentially hazardous conditions. In this study, dependence of hydrate growth on the reservoir temperature is examined to understand the behaviors of hydrate formation and deposition in a wellhead and to quantify the growth rate of hydrate deposition. It is found that insufficient convection and water condensation can delay hydrate deposition, with delayed growth, observed at the lower reservoir temperatures. Conversely, rapid growth of hydrate deposition with spike-like morphology are observed at the conditions inducing effective convection in the pipe and water condensation. The fugacity of water at the wall and center of each section of each pipe section is compared to understand the relationship between convection and water condensation. Significant hydrate formation was observed when the ratio of water fugacity at the wall and the center is lower than 0.5. Overall, this study provides further understanding with quantification and qualification of hydrate deposition behavior by considering the reservoir temperature.

## Keywords
wellhead; hydrate deposition; shut-in and restart

## Introduction
Gas hydrates are solid crystalline compounds formed by water and guest molecules, such as $CH_4$, $C_2H_6$, $C_3H_8$, $CO_2$, and $N_2$, under certain temperature and pressure [1]. Hydrate formation near the wellhead is of particular concern due to the possible plugging of the well tubing line, resulting in significant operational loss in additional of creating potentially hazardous conditions [2]. Especially, the shut-in and the eventual restart of a well represent the most concerning operation due to the favorable conditions for hydrate blockages. In a shut-in of a well, the top of the well up to the wellhead is gas-filled, and depending on the duration of the shut-in, the wellhead can be quickly cooled to ambient conditions, favoring the condensation of water at the top of the well or the pipe wall, which can lead to hydrate formation.
Accordingly, it has been conducted on how the header temperature, physical restriction, pipe size, geometry, and water vapor content impact on hydrate deposition [3-5]. Although previous studies have identified impact factors on hydrate deposition in wellhead, the comprehensive understanding of growth of hydrate deposition in wellhead has not been studied. To better understand and quantify the rate of hydrate formation in a wellhead, it is essential to collect reliable experimental data on hydrate formation using a wellhead model mimicking the conditions in a well tubing near the wellhead, or in a subsea flowline vertical riser.
In this study, the hydrate deposition process and morphology were examined with a focus on various reservoir and surrounding conditions representing the top of the well with warm fluids in the reservoir. Specifically, this study provides quantification of the amount of hydrate deposition as a function of time in different reservoir conditions.

## Methodology
The system includes a vertical upward pipe to mimic a well tubing near the wellhead as shown in Fig. (1). The reservoir is connected to a 1.21 m-long vertical straight pipe with 50 mm of inner diameter as a wellhead. The pipe has five individual 200 mm liquid-cooling sections with a 30 mm gap in-between. The gap is insulated with plastic foam. These sections are numbered 1 to 5 from top to bottom. The pipe is sealed at the top with a polycarbonate window, which allows direct visual observation and mounting a camera to monitor hydrate deposition. The light inside the pipe from the side windows of the 3 sections from the top is shown (section 1: white, section 2: red, and section 3: blue). The pipe is connected to a header with 6.0 L capacity at the bottom, which is filled with 3.0 L of deionized water. The header is equipped with a ceramic heater and an impeller to generate a temperature gradient in the system and

supply water into the pipe. Several intrusive resistance temperature detectors (RTDs, Omega® PT100 PR-17 series, USA) with an accuracy of ± 0.2 °C are located at each section to measure the center and wall temperatures of the pipe and the water reservoir. A pressure transducer (A-10, Wika, Germany) with 0.5% accuracy is used.

The hydrate deposition is characterized by a series of experiments with deionized water and $CH_4$ + $C_2H_6$ (75/25 mol%) provided by General Air, USA. The hydrate equilibrium temperature (HET) for this system is calculated using PVTsim® Nova 5.0 (SRK Peneloux, HV). Hydrate formation is initiated by controlling wall temperature ($T_w$) at given conditions of system pressure and reservoir temperature ($T_r$). The impeller is set at 500 RPM for a uniform temperature distribution in the reservoir. The hydrate deposition is represented by growth of hydrate formed in the wellhead. We monitored the hydrate growth under various conditions and quantified growth of hydrate deposition by the thickness of hydrate deposition. More detailed descriptions of the experimental apparatus and procedure can be found in previous studies [2-5].

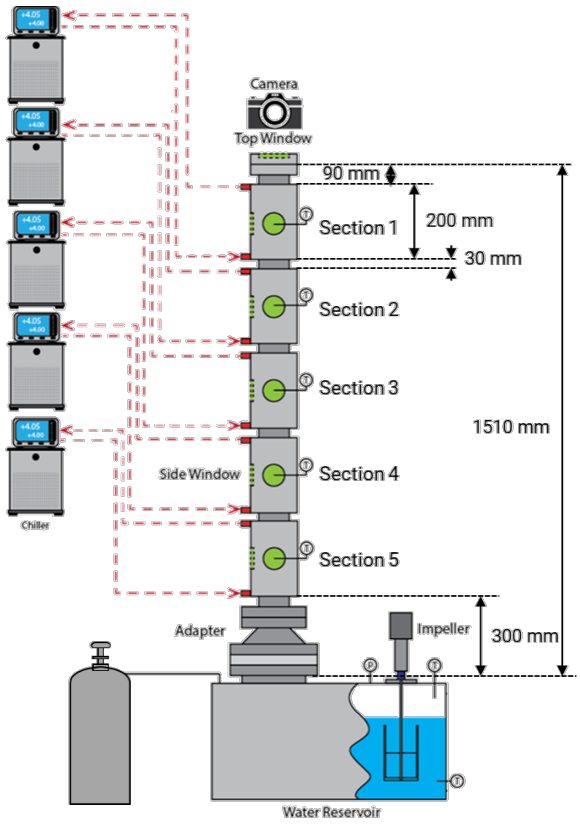


Figure 1. Schematic illustration of experimental setup.

## Results and Discussion

A series of tests was performed to examine the impact of the water reservoir temperature ($T_r$) on the hydrate deposition in the wellhead. The experiments were performed at $T_r$ = 60 °C (exp #1), 45 °C (exp #2), and 35 °C (exp #3). The wall temperature ($T_w$) was kept at $T_{w,1}$ = 0 °C (section 1), and 25 °C (section 3, 4, and 5). The temperature in section 2 was not controlled. As indicated in the Tab. 1, it was possible to observe hydrate formation in section 1 (top section) regardless of the reservoir temperature.

Table 1. Experimental conditions for hydrate deposition behavior by reservoir temperature.

| exp # | Pressure (bar) | Reservoir Temperature ($T_r$, °C) | Hydrate Formation (section) |
|---|---|---|---|
| 1 | 100 | 60 | Y (1) |
| 2 | 100 | 45 | Y (1) |
| 3 | 100 | 35 | Y (1) |

The pressure drop could indicate hydrate formation, and the pressure decreases 0.1880 bar/day in exp #1, 0.0961 bar/day in exp #2, and 0.0900 bar/day in exp #3 as shown in Fig. (2). The rate of pressure drop was higher in exp #1 and very similar for exp #2 and #3. This indicates that insufficient convection and water condensation can delay the rate of hydrate deposition, but hydrate deposition can be limited at the lower water reservoir temperature.

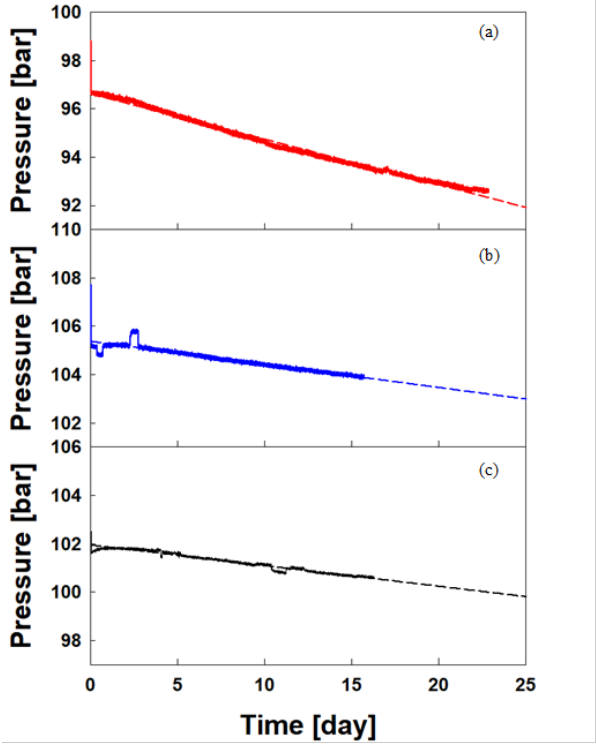


Figure 2. Pressure changes for (a) exp #1, (b) exp #2, and (c) exp #3.

Figure 3 shows hydrate deposition in terms of hydrate thickness. The hydrate growth rate varied to 0.8~1.9 mm/day during the first 5 days (0~5 days) depending on the conditions, and it was slowed down to 0.6~1.0 mm/day during the second 5 days (5~10 days). In exp #1, the growth of hydrate deposition was rapid at the beginning and decreased after several days. Exp #2 and #3

showed similar tendency, rapid initial growth and lower later, but the changes were not as drastic as in exp #1.

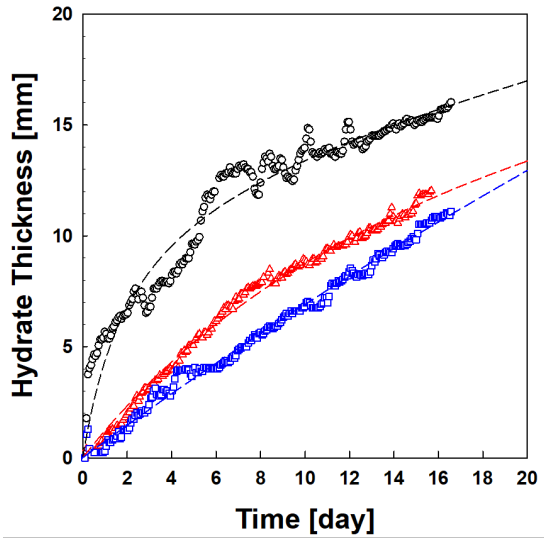


Figure 3. Hydrate deposit thickness with time for exp #1 (black circle), exp #2 (red triangle), and exp #3 (blue square). Dashed lines are the fitted curves.

Notably, the hydrate deposition rate in exp #3 seems to grow nearly linearly during the test time. The hydrate thickness (HT in mm) data were fitted to the following function:

$$HT = (A \times t) / (B + t) + C \times t \qquad (1)$$

where $t$ is time in day, and $A$, $B$, $C$ are fitted constants, which are listed below:

| | $A$ | $B$ | $C$ |
|---|---|---|---|
| exp #1 | 13.3526 | 2.2545 | 0.2497 |
| exp #2 | 28.1322 | 22.0610 | 0 |
| exp #3 | 102.6327 | 138.4633 | 0 |

The comparison with direct visual observation of the hydrate deposit also provides further understanding of the deposition process. Figure 4 shows observation from the top window at 0, 7, and 14 days for each experiment. Different light colors were used to identify the sections better. The visual observations clearly shows that the hydrate deposition grew slowly as the reservoir temperature decreased. Especially, the growing shape of hydrates was noticeable different. It was possible to observe spike-like (acicular) hydrate needles in exp #1, while the surface of the hydrate deposition was softer in exp #3. In the exp #2, the surface was rough but there was almost no spike-like deposition. These indicate that sufficient convection and water condensation causes rapid hydrate deposition with spike-like shape.

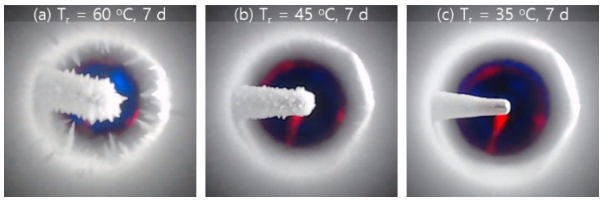


Figure 4. Visual observation from the top window after 7 days for exp #1 ($T_r$ = 60 °C, a), for exp #2 ($T_r$ = 45 °C, b), and for exp #3 ($T_r$ = 35 °C, c). Cool white, red, and blue lights are for sections 1, 2, and 3, respectively. As reference, the temperature probe (25 mm in length and 3 mm in diameter) is shown.

To understand the relationship between convection and water vapor condensation, the fugacity of water at the wall and center temperatures of each section was compared, as shown in Fig. (5). Fugacity is a corrected partial pressure or activity (effective concentration). Here, water fugacity shows how much water can condense from the gas to form hydrates.

Assuming that the vapor is water saturated at the center, $f_{w,wall}/f_{w,center}$ (red square) expresses water condensability at the wall. The $f_{w,wall}/f_{w,center}$ of sections 4 and 5 in exp #1 was lower than 1.0, and that in exp #2 were slight higher than that in exp #1 but still lower than 1.0, while that in exp #3 was almost 1.0. This indicates more water could be condensed in sections 4 and 5 in exp #1 than those in exp #2 and #3. However, in section 3, the $f_{w,wall}/f_{w,center}$ exceed 1.0 in all experiment conditions, and this allowed more water vapor to be transported upward the pipe in exp #1. In addition, unlike sections 4 and 5, section 2 showed lower $f_{w,wall}/f_{w,center}$ in exp #2 and #3 than exp #1. This restricted water convection through section 2 in exp #2 and #3, and this shows the growth of hydrate deposition is dependent on the convection of water vapor with sufficient driving force for hydrate formation.

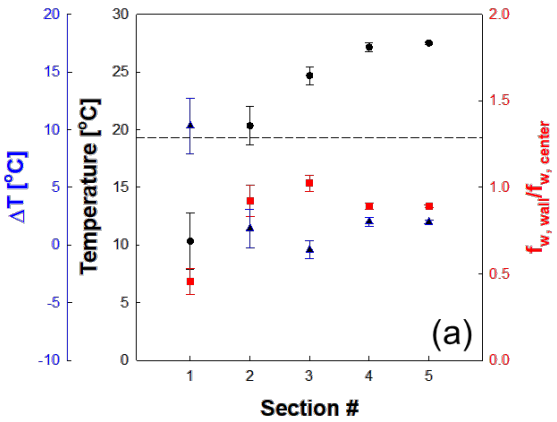

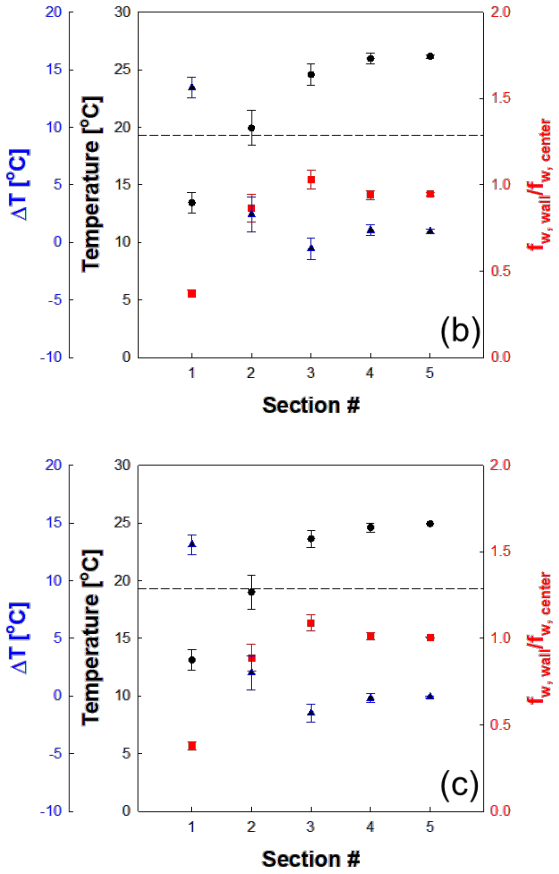


Figure 5. Comparison of fugacity of water at the wall and center temperatures of each section by reservoir temperature. (a) $T_r$ = 60 °C, (b) $T_r$ = 45 °C, and (c) $T_r$ = 35 °C.

## Conclusions

The characterization of hydrate deposition kinetics and morphologies is significant for developing safer design and operating guidelines for hydrate formation near the wellhead. This study investigates dependence of hydrate growth on the reservoir temperature to understand the behaviors of hydrate formation and deposition in a wellhead and to quantify the growth rate of hydrate deposition. It is found that insufficient convection and water condensation can delay hydrate deposition, with delayed growth, observed for the lower reservoir temperatures. Conversely, conditions inducing effective convection in the pipe and water condensation cause rapid growth of hydrate deposition with spike-like morphology. In order to understand the relationship between convection and water condensation, the fugacity of water at the wall and center of each section of each pipe section was compared. Water condensation started when the ratios of water fugacity at the wall and the center ($f_{w,wall}/f_{w,center}$) lower than 1.0, which indicates the vapor at the wall temperature is oversaturated, and hydrate wall deposition starts with the water condensation in the hydrate stable region. Significant hydrate formation was observed for $f_{w,wall}/f_{w,center}$ < 0.5. Overall, this study provides further understanding and data for hydrate deposition by considering the reservoir temperature. Also, the results have insight into better management strategies for hydrate formation near the wellhead.

## Acknowledgments

This work was funded by SaudiAramco.

## Responsibility Notice

The authors are the only responsible for the paper content.

## References

[1] Sloan, E.D.; Koh, C.A.; Clathrate Hydrates of Natural Gases, 3rd ed., CRC Press/Taylor & Francis, Boca Raton, 2008.

[2] Kinnari, K.J.; M. Askvik, K.; Li, X.; Austvik, T.; Zhang, X.; Sa, J.-H.; Lee, B.R.; Sum, A.K.; Hydrate Management of Deadlegs in Oil and Gas Production Systems – Background and Development of Experimental Systems, Energy Fuels, 31, 11783-11792, 2017.

[3] Zhang, X.; Lee, B.R.; Sa, J.-H.; Kinnari, K.J.; Askvik, K.M.; Li, X.; Sum, A.K.; Hydrate Management in Deadlegs: Effect of Header Temperature on Hydrate Deposition, Energy Fuels, 31, 11802-11810, 2017.

[4] Sa, J.-H.; Zhang, X.; Li, X.; Austvik, T.; Askvik, K.; Sum, A.K.; Hydrate management in deadlegs: Limiting hydrate deposition with physical restriction, Fuel, 270, 117506, 2020.

[5] Zhang, X.; Sa, J.-H.; Sum, A.K.; Hydrate management in Deadlegs: Effect of water vapor content on hydrate deposition, Fuel, 273, 117714, 2020.